Transmission electron microscopy and energy dispersive X-ray spectroscopy on the worn surface of nano-structured TiAlN/VN multilayer coating

LUO, Q. <http://orcid.org/0000-0003-4102-2129> and HOVSEPIAN, P. E. <http://orcid.org/0000-0002-1047-0407>

Transmission electron microscopy and energy dispersive X-ray spectroscopy on the worn surface of nano-structured TiAlN/VN multilayer coating

Q. Luo, P. Eh. Hovsepian

Materials and Engineering Research Institute, Sheffield Hallam University, Sheffield, S1 1WB, UK

Abstract

Nano-structured TiAlN/VN multilayer hard coatings grown by cathodic arc metal ion etching and unbalanced magnetron sputtering deposition have repeatedly shown low coefficients of friction and wear. In this paper, we employed the combined methods of cross-sectional ion beam milling sample preparation, conventional transmission electron microscopy, energy dispersive X-ray spectroscopy and quantitative spectrum analysis to give a comprehensive characterization of wear induced tribofilm, worn TiAlN/VN surface as well as wear debris. The major wear mechanism operating in the TiAlN/VN coating is the tribo-oxidation wear. A 20 – 50 nm thick tribofilm was observed on the TiAlN/VN worn surface, having inhomogeneous density, amorphous structure and multicomponent V-Al-Ti-O composition. Therefore the real sliding contact during the ball-on-disk test was a three-body sliding system including the tribofilm, in which the self-sintering and shearing deformation of the multicomponent oxide film played a significant role in determining the low friction coefficient. Owing to the low friction and high hardness, the TiAlN/VN worn surface retained good structural integrity without any crack, delamination or detectable deformation, resulting in minimized mechanical wear.

Key words: Transmission electron microscopy (TEM); Energy dispersive X-ray spectroscopy (EDXS); Tribology; TiAlN/VN multilayer coating

1. Introduction

TiAlN/VN multilayer coatings having a period of approximately 3 nm have been grown by unbalanced magnetron sputtering deposition and show extremely low dry sliding wear coefficient in the scale of 10^{-17} $m^3 \cdot N^{-1} \cdot m^{-1}$ [1 – 3]. The excellent tribological properties promise industrially valuable applications such as in cutting tools for coolant-free machining of aluminium alloys [4]. However, the wear mechanisms operating in the TiAlN/VN coatings are not fully understood up to date.

It is well known that wear mechanisms in physical vapour deposited (PVD) coatings, including abrasion, fatigue wear, cohesive and adhesive spalling, and tribo-oxidation wear, depend on the applied tribological conditions and on the mechanical and chemical properties. In the TiAlN/VN coatings, the low wear coefficient is related to several factors such as the high hardness, the low friction coefficient in a range of 0.4 – 0.6, and the oxidation behaviour. The extraordinarily high hardness in nano-scale multilayers of transition metal nitrides, e.g. $HK_{0.025}$ 30 – 50 GPa in the TiAlN/VN, is attributed to several hardening mechanisms, namely the different shear modulus between the multilayer phases, the coherent strain, and the high density of coherent boundaries [5 - 7]. Our previous transmission electron microscopy (TEM) study on a similar multilayer nitride TiAlN/CrN has revealed that nano-scale structure possesses higher resistance against worn surface deformation than the monolithically grown hard coatings and therefore can significantly reduce the scale of abrasion, crack generation and delamination wear [8, 9].

In parallel, the friction coefficient of the TiAlN/VN coatings is substantially lower than those of other TiN- and TiAlN-based hard coatings [2], which is also beneficial to the low wear coefficient. Concerning the friction mechanism operating in the TiAlN/VN, previous Raman microscopic analysis has found a tribo-oxidation product V_2O_5 in the wear debris [10]. As V_2O_5 is reported to have low melting point and good solid lubricity [11, 12], it has been speculated that the low friction coefficient of TiAlN/VN is attributed to the formation of V_2O_5 oxide. In a recent

iso-thermal annealing experiment, however, the oxidation of the TiAlN/VN coatings was found to generate not only V_2O_5 but also other types of oxides such as $AlVO_4$, TiO_2 and Al_2O_3 [13, 14]. The influence of these oxides was not considered in the above speculation. Moreover, considering the different conditions between the static iso-thermal oxidation and the dry sliding wear, an even closer approach can be gained by direct observation and characterization of the worn samples themselves.

Tribo-oxidation occurs in the wear of metals and non-oxide ceramics in most atmospheric circumstances. As a general tribological phenomenon, the combined mechanical and chemical interactions between the coupled sliding surfaces and the environment lead to the formation of a nano-scale or sub-micron scale tribofilm, which in turn has a strong impact on the friction and wear performance [15, 16]. The characterization of tribofilms has attracted studies using many sophisticated analytical techniques [15 - 18]. In particular, TEM is especially useful owing to its higher spatial resolution than other micro-analyses and to its multiple approaches of imaging, diffraction and spectrometry [9, 17 - 19]. In this paper, we report the latest cross-sectional TEM observation and quantitative energy dispersive X-ray spectroscopy (EDXS) of a nano-scale tribofilm formed on the worn surface of TAlN/VN coating. The research is aimed to achieve a deeper understanding in the microstructure aspects of the wear mechanisms.

2. Experimental details

TiAlN/VN coating was grown on polished steel coupons using a four-target unbalanced magnetron reactive sputtering system. Two turbomolecular pumps (2200 $l \cdot s^{-1}$ each) provide a base pressure of 1×10^{-6} mbar. The following target materials were used for the coating deposition: two target pairs of TiAl (50:50 at%) and V (99.8 % pure) targets opposing each other to form TiAlN/VN. Detailed deposition procedure can be found in refs. [1 – 3]. The sample surface was pre-etched by highly energetic vanadium ions in cathodic arc mode. Then the system

was operated under sputtering mode to deposit a 0.3 μm thick VN base layer followed by a 3 μm thick TiAlN/VN multilayer, both under a substrate bias voltage -75 V and temperature 450^{o}C. The deposition process was controlled in total pressure mode (P_{Ar}:P_{N2} = 50:30, P_{Ar} + P_{N2}= constant) in a common Ar+N_2 atmosphere to achieve stoichiometric nitride composition [20, 21]. The TiAlN and VN bi-layer thickness in the TiAlN/VN was determined to be 3.02 nm by using cross-sectional TEM imaging [22].

The friction and wear property was determined using a pin-on-disc tribometer at conditions of room temperature 20 – 30 ^{o}C, dry sliding at relative humidity 30 – 40 %, using a 6 mm in diameter Al_2O_3 ball counterpart, applied normal load 5 N, linear sliding speed 0.1 m·s^{-1}, and total sliding duration 200,000 laps (leading to a sliding distance 9.0 km). The long term sliding resulted in a wear track on the TiAlN/VN to be approximately 0.4 mm in width and less than 0.5 μm in depth. Detailed mechanical and tribological evaluation has been published elsewhere [22].

Cross-sectional TEM specimens containing the obtained worn surface were sectioned from the tested sample using a high-speed SiC disc saw, and thinned from both cross-section sides by metallographic grinding and polishing to a thickness of 20 – 30 μm. The thinned specimen was then glued to a 3 mm copper grid having a 1 mm × 2 mm slot-hole and further thinned to electron transparency by argon ion beam milling. A two-cathode Gatan precision ion polish system was used in the ion beam milling. The instrument was operated in such a modulator model that ion beam is only allowed to bombard the specimen following a direction from the back towards the worn surface edge. The front worn surface edge therefore was placed in a shadow position free from any ion beam damage. The shadowing effect, however, leads to simultaneous re-deposition of ion-sputtering removed species (mostly from the copper grid as well as a small portion from the sample substrate) on the outmost worn surface. The copper re-deposit, which is clearly visible in TEM observation (to be shown later), then serves as a guide in recognizing the worn surface.

In addition to the above, wear debris attached besides the wear track was collected on a carbon film 200-mesh copper grid for direct access to TEM.

All the TEM analyses were performed on a 200 kV Philips STEM-CM20 instrument with a LaB_6 filament and an attached EDXS system. The EDXS facility comprises an ultra-thin window X-ray detector and a Link ISIS computer system (The Oxford Instruments plc). Conventional TEM characterization techniques utilized in this study included bright field (BF) imaging, dark field (DF) imaging, selected area electron diffraction (SAED), convergent beam electron diffraction and EDXS quantitative analysis. For the EDXS analysis, only extremely thin areas were used to acquire spectrum in order to reduce the absorption of low-energy signals such as O-K_α and N-K_α. In each of the acquired spectrum, the Cliff-Lorimer ratio technique [23] was employed to calculate the composition using net peak integrations of V-K_α, Ti-K_α, Al-K_α and O-K_α. Considering the over-lapping between V-K_α and Ti-K_β and between O-K_α and V-L_α, the Ti-K_β and V-L_α counts were taken off to get the net counts of V-K_α and O-K_α respectively, where the ratios [Ti-K_β]/[Ti-K_α] and [V-L_α]/[V-K_α] were estimated following TEM-EDXS calibrations using a vanadium-free TiAlN coating specimen (not shown here) and the VN base layer. Of the three factors used in the Cliff-Lorimer calculation, both the absorption and fluorescence factors can be ignored for the high energy K_α of metals in case of the thin TEM sample. The Z factors were estimated to be $k_{Ti/Al}$ = 1.422 (calibrated from a $Ti_{0.5}Al_{0.5}N$ TEM foil) and $k_{V/Al}$ = 0.93 according to ref. [24]. However, as the thickness-related absorption of O-K_α could not be quantified, the oxygen content was estimated in a lower precision as compared to the metal contents. The factor $K_{O/Al}$ = 1.51 was determined on a pure α-Al_2O_3 sample.

3. Results

The TiAlN/VN coating exhibited an average surface roughness of R_a 0.341 μm, hardness $HK_{0.025}$ 28.3 GPa and scratch critical load L_c 55.6 N [23]. Fig. 1 shows the dry sliding friction coefficient curve. The friction curve started at a value 0.219 and, after a running-in period, became stable at approximately 0.4. The measured mean value and standard deviation of the friction coefficient were 0.400 and 0.0018 respectively. This is consistent to our previous reports in which the TiAlN/VN coatings showed repeatedly low friction coefficient in a range $\mu = 0.4 – 0.6$ [1, 2, 23]. By the end of the test a wear track depth as small as 0.3 μm was created, leading to the overall wear coefficient $K_c = 2.3 \times 10^{-17}$ $m^3 \cdot N^{-1} \cdot m^{-1}$.

Fig. 2a shows a scanning back-scattered electron micrograph of as-deposited TiAlN/VN surface. The surface morphology is featured by the presence of droplet-induced growth defects and surface grooves. As a general phenomenon happening in acthodic arc, metal droplets were emitted to reach and deposit on the substrate surface, each leading to a localized growth defect. Meanwhile, the original roughness of the pre-polished substrate surface was modified as a result of the applied metal ion etching. Consequently, the grooves observed on the coating surface resulted from the preferential etching of the substrate steel. The applied bias voltage during the coating deposition also played a role in determining the surface roughness, which has been characterized by atomic force microscopy and cross-sectional TEM [22]. In Fig. 2b, the worn surface is even smoother than the as-deposited coating owing to the removal of defects and surface grooves. More importantly, the worn surface, even in the areas of the preferential wear of the droplet defects (see the black holes in the image), does not show any crack or visible delamination wear. More details of the friction and wear property can be found in ref. [23].

A pair of TEM BF and DF micrographs (Figs. 3a and 3b) show the cross-sectional structure of the worn TiAlN/VN coating. The upper part in the micrographs, marked as ‘I’ in the micrographs, is a portion of the copper re-deposit resulted from the ion beam milling, which has been confirmed by EDXS analysis. Beneath the copper re-deposit is the outmost worn surface

edge where a tribofilm (marked as 'II') can be seen to show a thickness ranging in 20 – 40 nm and a clear boundary to the adjacent TiAlN/VN coating (marked as 'III'), seen at higher magnification in Fig. 3c. The tribofilm seems to be more transparent than the adjacent TiAlN/VN. It is amorphous, as its convergent beam electron diffraction showed only a transmission (central) spot and it exhibited a constantly 'grey' diffraction contrast (Figs. 3a and 3b) not changing with sample tilting. In the area exactly below the tribofilm, the TiAlN/VN coating retains its regular multilayer fringes, see Fig. 3c. The curvature in the multilayer fringes was attributed to the applied low substrate bias voltage (-75V) which led to a rough growth surface [22]. In previous research, we have found that worn surface deformation induced by high load and high friction in sliding wear leads to crack generation and delamination wear of transition metal nitride coatings like TiN, TiAlCrN and TiAlN/CrN. However, the TiAlN/VN coating presented in this work exhibits no measurable deformation up to the instrumental spatial resolution of TEM, no occurrence of crack or delamination wear.

Fig. 4 shows typical EDX spectra taken at a spot size of 15 nm in nominated diameter in the following areas: (a) copper re-deposit layer, (b) tribofilm, (c) wear debris (to be shown later in Fig. 5), (d) TiAlN/VN coating close to the worn surface, and the VN base layer (image not shown here but given in ref. [22]). The spectrum taken in the re-deposit layer indicates merely the sputtered material from the copper grid and sample substrate. The spectrum from the tribofilm area shows high intensity peaks of V-K_α (4.95 keV), Ti-K_α (4.51 keV) and Al-K_α (1.49 keV), and a small but distinct peak O-K_α. It is also noted that the N-K_α channel (0.39 keV) locates exactly at the valley position. In addition, there are overlaps of the V-K_α with the Ti-K_β (4.932 keV) and of the O-K_α with V-L_α (0.51 keV). The Cu peaks are due to sample drift to the adjacent copper layer because of the extremely small thickness of the tribofilm, 20 – 40 nm. Similar results are obtained in the wear debris. Thus the tribofilm and wear debris are predominately a mixture of multi-component oxide V-Al-Ti-O. The spectrum from the TiAlN/VN area shows high intensity

peaks V-K_α, Ti-K_α and Al-K_α, and a distinct peak N-K_α. An example spectrum collected in the VN base layer is also given for the purpose of V-L_α/K_α ratio calibration.

The TEM-EDXS qualitative analysis indicates that the tribofilm is predominately a mixture of oxide and the coating adjacent to the tribofilm has kept the TiAlN/VN composition containing negligible oxygen. In previous research, we have found that the iso-thermal oxidation of a TiAlN based multicomponent coating led to the formation of a 50 nm thick transition layer where nitride transformed progressively to oxide [25]. This is clearly not the case in the tribo-oxidation. Figs. 3 and 4 suggest that a sharp boundary exists between the tribofilm and the TiAlN/VN without any detectable intermediate layer.

Spectrum quantification has been carried out for the EDXS results obtained in the tribofilm and the adjacent TiAlN/VN respectively, Tables 1 and 2. The average compositions are determined from four to five measurements as presented. In Table 1, the average composition of the TiAlN/VN coating was determined to be 15.9 at%Al, 15.3 at%Ti and 18.8 at%V assuming a stoichiometric content of nitrogen (50 at%N). In Table 2, the chemical composition of the tribofilm was determined to be 36.8 at%O, 19.6 at%Al, 19.9 at%Ti and 23.8 at%V. The oxygen content is however, of lower precision because of the large scattering in the oxygen content (between 24.3 at% and 46.1 at%, giving a standard deviation 9.8 at%) due to the un-corrected absorption of both O-K_a and V-L_a. The real oxygen content could be even higher. Nevertheless, the composition reveals considerable amount of oxygen and co-existence of Al, Ti and V, indicating a multi-component oxide mixture V-Al-Ti-O. In particular, it exhibits similar metal-to-metal ratios, i.e. Al:Ti = 0.98 and V:Ti = 1.19, as compared to the TiAlN/VN (being 1.04 and 1.22 respectively).

From Tables 1 and 2, it is noticed that the tribofilm emitted substantially lower intensity and higher data scattering of specific X-rays (e.g. V-K_α = 2489 ± 1009 counts) than the TiAlN/VN

coating (e.g. V-K_α = 5308 ± 380 counts). Noting the identical acquiring conditions applied in both areas, the lower intensity suggests significantly lower mass density in the tribofilm. In TEM imaging, an area of low mass density is expected to give high brightness in zero-loss imaging or bright-field imaging due to less amount of inelastic electron scattering. This has been confirmed in Fig. 3 which shows brighter contrast in the tribofilm area than the adjacent TiAlN/VN. The data scattering of K_α peaks in Table 2 might further imply that the tribofilm is inhomogeneous to nano-scale.

Fig. 5 shows TEM analyses of TiAlN/VN wear debris. In Fig. 5a, the bright field micrograph shows clusters of amorphous debris. The amorphous structure is also revealed by the broad diffusive rings in the SAED pattern, Fig. 5b. In addition, the three distinct diffraction rings in Fig. 5b suggests that crystalline α-Al_2O_3 particles exist in the debris as a result of the wear of the alumina counterpart. However, the wear coefficient of the counterpart, $K_{ball} = 4 \times 10^{-19}$ $m^3 \cdot N^{-1} \cdot m^{-1}$ [23], is so small that accounted for only 1.8% that of coating ($K_{coat} = 2.3 \times 10^{-17}$ $m^3 \cdot N^{-1} \cdot m^{-1}$). Therefore the majority of the wear debris comes from the wear of the coating. A typical EDX spectrum of the wear debris is shown in Fig. 4. By carefully identifying the energy channel position of N-K_α and O-K_α, it has been found that O-K_α dominated the intensity peak and N-K_α position is close to the valley. The debris is consequently considered to be free from nitrogen, which means that non-detectable amount of nitrides indicate negligible mechanical wear of the coating. More details of the EDXS analysis results are shown in Table 3. The composition of the wear debris was determined to be 44.9 at%O, 17.2 at%Al, 17.6 at%Ti and 20.3 at%V. This is close to the composition of the tribofilm as shown in Table 2.

4. Discussion

The low friction coefficient of TiAlN/VN coating presented in Fig. 1 is consistent with our previous research [1, 2, 23]. Low friction resulted in a smooth and delamination-free worn surface (Fig. 2). Innovative contribution in this paper is the cross-sectional TEM presentation and characterization of a nano-scale oxide film on the worn surface.

The observed tribofilm is 20 – 50 nm thick, amorphous and closely attached to the TiAlN/VN with a distinct interface, Fig. 3. The tribofilm is almost free of nitrogen and exhibits a chemical composition of 36.8 at%O, 19.6 at%Al, 19.9 at%Ti and 23.8 at%V, Table 2. In parallel, good agreement can be seen between the tribofilm and wear debris except the uncertainty in oxygen content. The current EDXS results suggest that the tribofilm and wear debris are mainly generated from the wear of the coating although the debris did show the presence of Al_2O_3 nano-particles. Such tribofilm is different from the film generated in the wear of TiN and TiAlN based coatings sliding against a steel counterpart where the tribofilm and debris were both nano-crystalline iron oxides [9, 26, 27]. Similar amorphous structures in wear debris or in tribofilms have been reported in ref. [16, 17, 27]. Although the oxygen content determined is still in low precision, the results presented have suggested that EDXS analysis on ion-beam milling thinned TEM foil is an appropriate method to distinguish light elements like oxygen and nitrogen, especially when locating the electron probe close to the extremely thin edge.

A schematic diagram (Fig. 6) can be drawn to show the formation of tribofilm. As soon as wear debris is generated, it is involved in the sliding wear by forming a tribofilm between the contacting surfaces. The tribofilm reported in this study neither has a crystalline structure as compared to the annealing induced oxides of TiAlN/VN [13, 14], nor contains crystalline V_2O_5 as reported in previous Raman microscopy study [10]. However, it really resulted in a three-body system: the counterpart, tribofilm and the coating. In particular, the amorphous structure revealed that the tribofilm would have experienced severe shear straining in each pass of the pin-on-disc contact and therefore, it was the shearing resistance of the multi-component oxide film which

determined the low-value and stable friction coefficient of the TiAlN/VN. A deeper understanding of the composition and ionic structure is proposed, for example, by electron energy loss spectroscopy study. Nevertheless, it is indicated that a low friction coefficient favours low rate of tribo-oxidation wear. In literature [28], the friction induced bulk temperature and flash temperature in dry sliding wear of metals were described to increase linearly with increasing friction coefficient. Therefore in the current experiments, the low friction coefficient of TiAlN/VN ($\mu = 0.4$) is expected to lead to low increase of temperature within the sliding contact zone as compared to the sliding wear of high-friction coating TiAlCrYN ($\mu = 0.66$ [23]). As a temperature dependent process, the oxidation of the coating at the tribofilm-nitride interface is expected to be an extremely slow process.

In addition, the cross-section TEM observations confirmed good integrity of the TiAlN/VN multilayer up to the outmost worn surface (Fig. 3) which forms a big contrast to our previous observations of the wear induced deformation and coating delamination occurring in TiN, TiAlN/CrN and TiAlCrYN coatings [8, 9, 26]. This implies a negligible amount of mechanical wear.

5. Conclusions

In dry sliding wear tests, TiAlN/VN coatings deposited by cathodic arc metal ion etching and unbalanced magnetron sputtering deposition have repeatedly shown low coefficients of friction and wear. In this paper, results have been presented on TEM observation and associated EDXS analysis of worn surface and wear debris, leading to the following conclusions.

A 20 – 50 nm thick tribofilm was observed on the TiAlN/VN worn surface. Both the tribofilm and the wear debris showed inhomogeneous density, amorphous structure and multicomponent

V-Al-Ti-O composition. The tribofilm was formed through a self-sintering process of oxide wear debris involved between the sliding surfaces.

Crystalline V_2O_5 oxide was not found on the worn surface or in the debris. Therefore, it was the multicomponent V-Al-Ti-O oxide, instead of the lubricious V_2O_5, which determined the low friction coefficient.

The major wear mechanism operating in the TiAlN/VN coating is the tribo-oxidation wear. The TiAlN/VN worn surface exhibited good structural integrity without any crack, delamination or detectable deformation, resulting in minimized mechanical wear.

The employed cross-sectional TEM and EDXS method on ion-beam thinned samples is capable of observing nano-scale oxide film and distinguishing the light elements oxygen and nitrogen whereas the EDXS for metals are fully quantitative.

References

[1] WD Münz, LA Donohue, PEh Hovsepian, Surf. Coat. Technol. 125 (2000) 269.

[2] PEh Hovsepian, DB Lewis, WD Münz, Surf. Coat. Technol. 133-134 (2000) 166.

[3] PEh Hovsepian, WD Münz, Vacuum 69 (2003) 27.

[4] Q Luo, G Robinson, M Pittman, M Howarth, WM Sim, MR Stalley, H Leitner, R Ebner, D Caliskanoglu, PEh Hovsepian, Surf. Coat. Technol. 2005, to be published.

[5] JS Koehler, Phys. Rev. B2 (1970) 547.

[6] U Helmersson, S Todorova, SA Barnett, JE Sundgren, LC Markert, JE Greene, J. Appl. Phys. 62 (1987) 481.

[7] SA Barnett, M Shinn, Annu. Rev. Mater. Sci. 20 (1990) 245.

[8] Q Luo, WM Rainforth, WD Münz, Wear 225-229 (1999) 74.

[9] Q Luo, WM Rainforth, WD Münz, Scripta Mater. 45 (2001) 399.

[10] CP Constable, J Yarwood, PEh Hovsepian, LA Donohue, DB Lewis, WD Münz, J. Vac. Sci. Technol. A18 (2000) 1681.

[11] PH Mayrhofer, PEh Hovsepian, WD Mitterer, Surf. Coat. Technol. 177-178 (2004) 341.

[12] A Erdemir, Tribo. Lett. 8 (2000) 97.

[13] DB Lewis, S Creasey, Z Zhou, JJ Forsyth, AP Ehiasarian, PEh Hovsepian, Q Luo, WM Rainforth, WD Münz, Surf. Coat. Technol. 177-178 (2004) 252.

[14] Z Zhou, WM Rainforth, DB Lewis, S Creasey, JJ Forsyth, F Clegg, AP Ehiasarian, PEh Hovsepian, WD Münz, Surf. Coat. Technol. 177-178 (2004) 198.

[15] A Erdemir, C Bindal, GR Fenske, Appl. Phys. Lett. 68 (1996) 1637.

[16] M Woydt, A Skopp, I Dorfel, K Witke, Wear 218 (1998) 84.

[17] A Blomberg, S Hogmark, J Lu, Tribo. Int. 26 (1993) 369.

[18] C Minfray, JM Martin, C Esnouf, T Le Mogne, R Kersting, B Hangenhoff, Thin Solid Films 447-448 (2004) 272.

[19] WM Rainforth, R Stevens, J Nutting, Phil. Mag. A66 (1992) 621.

[20] LA Donohue, WD Münz, DB Lewis, J Cawley, T Hurkmans, T Trinh, I Petrov, JE Greene, Surf. Coat. Technol. 93 (1997) 69.

[21] DB Lewis, LA Donohue, M Lembke, WD Münz, Jr. R Kuzel, V Valvoda, CJ Blomfield, Surf. Coat. Technol. 114 (1999) 187.

[22] Q Luo, DB Lewis, PEh Hovsepian, WD Münz, J. Mater. Res. 19 (2004) 1093.

[23] Q Luo, PEh Hovsepian, DB Lewis, WD Münz, YN Kok, J Cockrem, M Bolton, A Farinotti, Surf. Coat. Technol. 193 (2005) 39.

[24] DB Williams, CB Carter, Transmission electron microscopy IV: Spectrosmetry. New York: Plenum Press; 1996. p. 608.

[25] Q Luo, C Leyens, P Eh Hovsepian, D B Lewis, C P Constable, WD Münz, Oxidation mechanism of PVD TiAlCrYN coating observed by analytical TEM, Electron Microscopy and Analysis 2001, edt. M. Aindow and C.J. Kiely, Institute of Physics, 2001, p. 369.

[26] Q Luo, WM Rainforth, WD Münz, Surf. Coat. Technol. 146-147 (2001) 430.

[27] E de Wit, B Blanpain, BL Froyen, JP Celis, Wear 217 (1998) 215.

[28] SC Lim, MF Ashby, Acta. Metall. 35 (1987) 1.

Table and figure captions

Table 1 The chemical composition of TiAlN/VN coating determined by quantitative TEM-EDXS analysis. *The N content is assumed to be 50 at% for the stoichiometric nitride coating.

Table 2 The chemical composition of tribofilm determined by quantitative TEM-EDXS analysis.

Table 3 The chemical composition of wear debris determined by quantitative TEM-EDXS analysis.

Fig. 1 Friction curve of TiAlN/VN coating.

Fig. 2 Back-scattered scanning electron micrographs of TiAlN/VN coating. (a) as-deposited coating surface; (b) Worn surface after 200,000 laps of dry sliding against an alumina ball at 5N, 0.1 $m \cdot s^{-1}$.

Fig. 3 Cross-sectional TEM BF images of worn TiAlN/VN coating showing the copper re-deposit (marked as region I), a tribofilm (region II), and the TiAlN/VN multilayer coating (region III). (a) Low-magnification BF image; (b) Associated DF image; and (c) High-magnification BF image.

Fig. 4 Typical EDX spectra obtained in the cross-section TEM sample. (a) In the copper re-deposit; (b) In tribofilm; (c) In loose wear debris (see Fig. 5a); (d) In TiAlN/VN close to the tribofilm; and (e) In the VN base layer.

Fig. 5 TEM analysis of wear debris: (a) a bright field micrograph and (b) a SAED pattern.

Fig. 6 Schematic graph showing the formation of tribofilm and its influence on the wear of coating.

Tables

Table 1 The chemical composition of TiAlN/VN coating determined by quantitative TEM-EDXS analysis. *The N content is assumed to be 50 at% for the stoichiometric nitride coating.

	Peak integration [unit: counts]			Estimated Composition [unit: at%]			
	Al-K_α	Ti-K_α	V-K_α	N*	Al	Ti	V
Range [keV]	1.33 – 1.61	4.33 – 4.69	4.75 – 5.13				
Spectrum 1	2076	2475	4981	50	15.9	15.2	18.9
Spectrum 2	2144	2440	4879	50	16.5	15.0	18.5
Spectrum 3	2090	2768	5309	50	15.1	16.0	18.9
Spectrum 4	2392	2822	5652	50	16.1	15.2	18.7
Spectrum 5	2378	2793	5717	50	16.0	15.1	18.9
[Mean] ± [deviation]	2216 ± 156	2660 ± 186	5308 ± 380	50	15.9 ± 0.51	15.3 ± 0.41	18.8 ± 0.17

Table 2 The chemical composition of tribofilm determined by quantitative TEM-EDXS analysis

	Peak integration [unit: counts]				Estimated Composition [unit: at%]			
	O-K_α	Al-K_α	Ti-K_α	V-K_α	O	Al	Ti	V
Range [keV]	0.39 – 0.65	1.33 – 1.61	4.33 – 4.69	4.75 – 5.13				
Spectrum 1	740	730	889	1553	46.1	17.8	17.4	18.7
Spectrum 2	678	1021	1269	2717	42.7	17.2	18.4	21.7
Spectrum 3	710	729	977	1873	33.9	20.0	19.9	26.2
Spectrum 4	629	1524	1975	3811	24.3	23.2	24.0	28.5
[Mean] ± [deviation]	689 ± 47	1001 ± 374	1278 ± 493	2489 ± 1009	36.8 ± 9.8	19.6 ± 2.7	19.9 ± 2.9	23.8 ± 4.4

Table 3 The chemical composition of wear debris determined by quantitative TEM-EDXS analysis

	Peak integration [unit: counts]				Estimated Composition [unit: at%]			
	O-K_α	Al-K_α	Ti-K_α	V-K_α	O	Al	Ti	V
Range [keV]	0.40 – 0.65	1.32 – 1.64	4.33 – 4.69	4.77 – 5.15				
Spectrum 1	2535	2365	2667	5368	44.1	18.5	16.7	20.7
Spectrum 2	1660	1310	1638	3335	46.6	16.4	16.4	20.6
Spectrum 3	1519	1370	1547	2844	46.2	18.4	16.6	18.8
Spectrum 4	1266	1126	1526	2755	43.1	17.3	18.7	20.8
Spectrum 5	3631	2817	4460	7689	44.3	15.4	19.5	20.8
[Mean] ± [deviation]	2122 ± 969	1798 ± 747	2368 ± 1263	4398 ± 2122	44.9 ± 1.5	17.2 ± 1.3	17.6 ± 1.4	20.3 ± 4.3

Figure 1

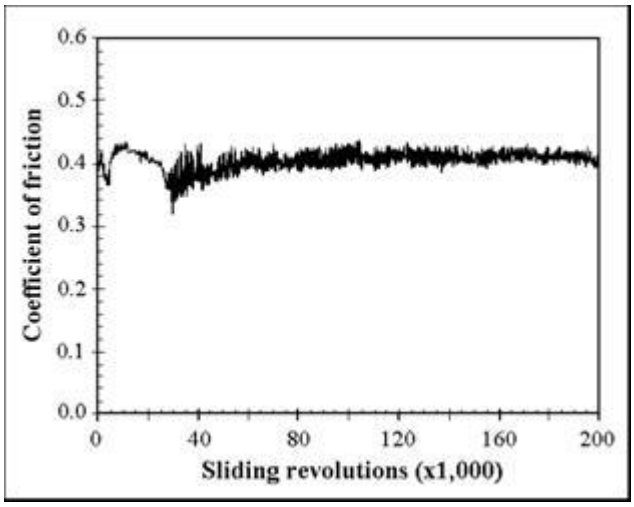
Coefficient of friction
0.6
0.5
0.4
0.3
0.2
0.1
0.0
0
40
80
120
160
200
Sliding revolutions (x1,000)

Figure 2

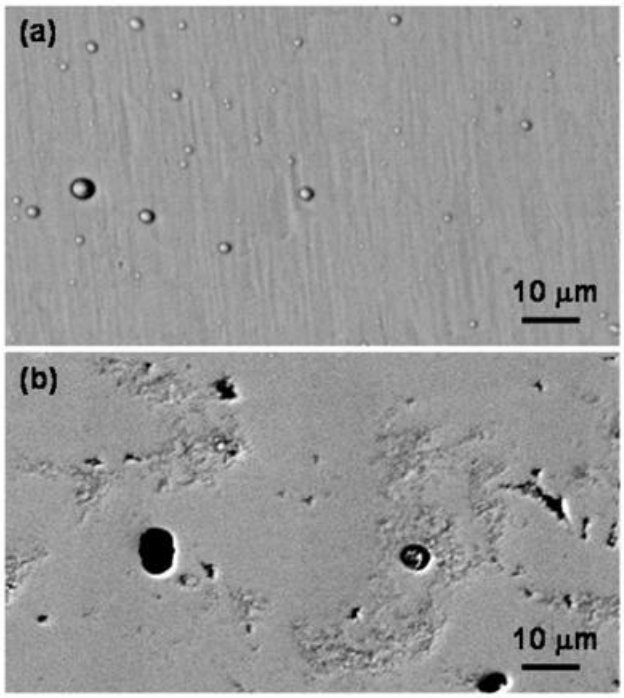

Figure 3a / Figure 3b

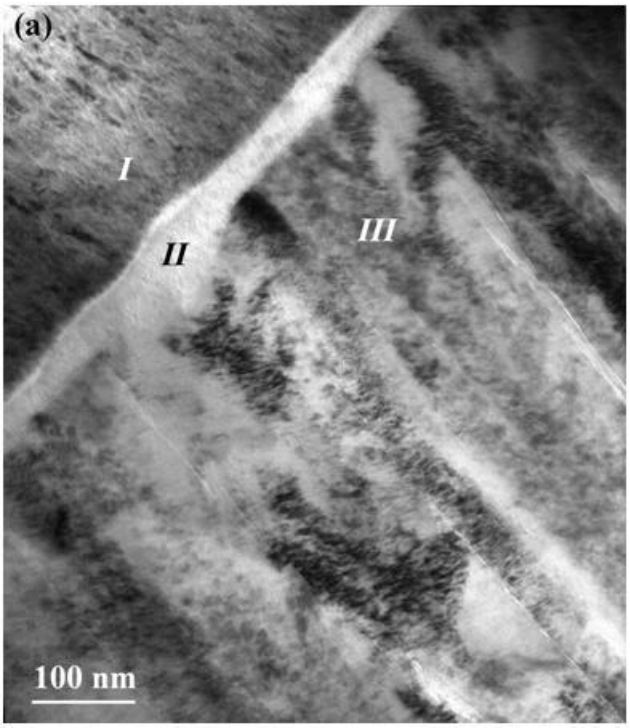

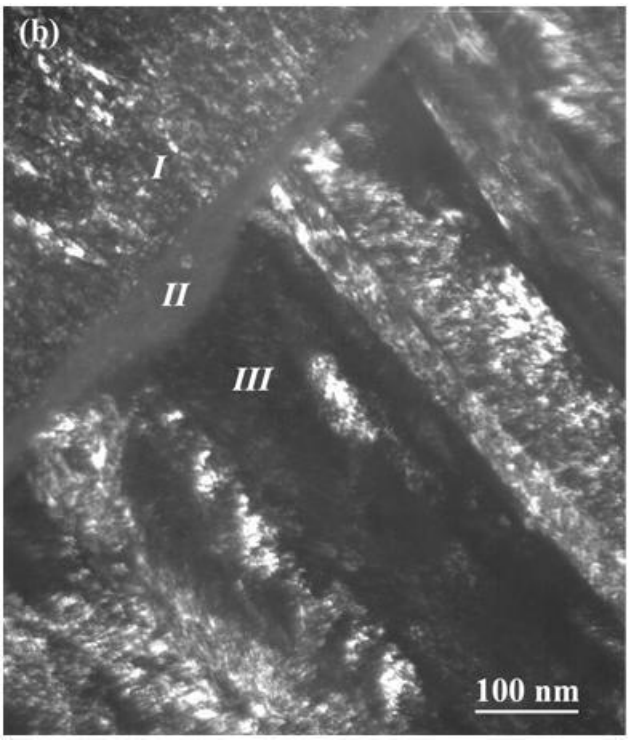

Figure 3c

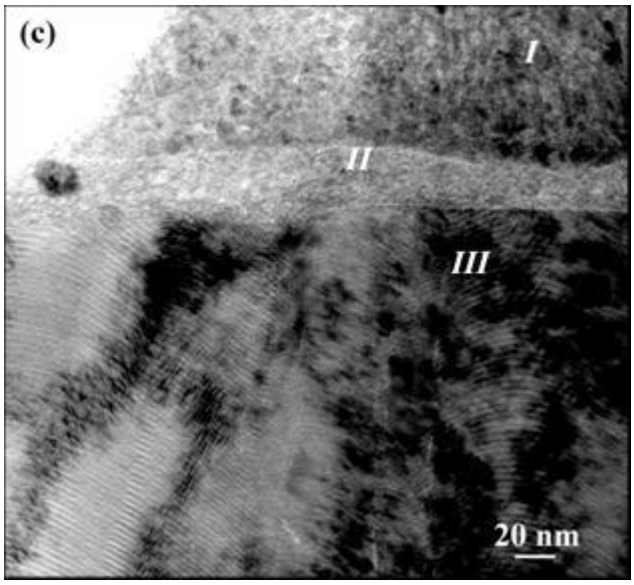

Figure 4

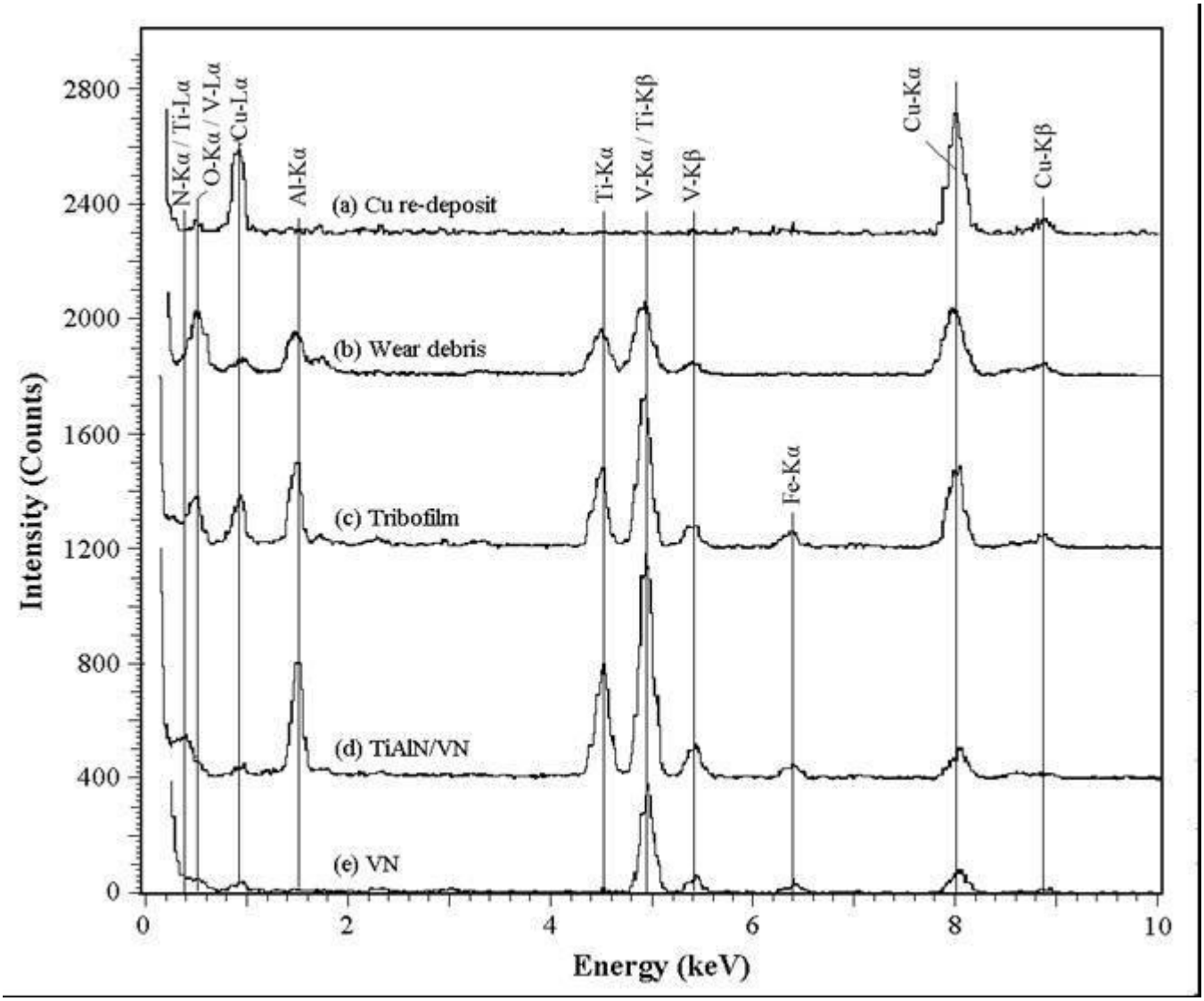
N-Kα / Ti-Lα
O-Kα / V-Lα
Cu-Lα
Al-Kα
Ti-Kα
V-Kα / Ti-Kβ
V-Kβ
Fe-Kα
Cu-Kα
Cu-Kβ
(a) Cu re-deposit
(b) Wear debris
(c) Tribofilm
(d) TiAlN/VN
(e) VN
Intensity (Counts)
Energy (keV)
0
400
800
1200
1600
2000
2400
2800
0
2
4
6
8
10

Figure 5a

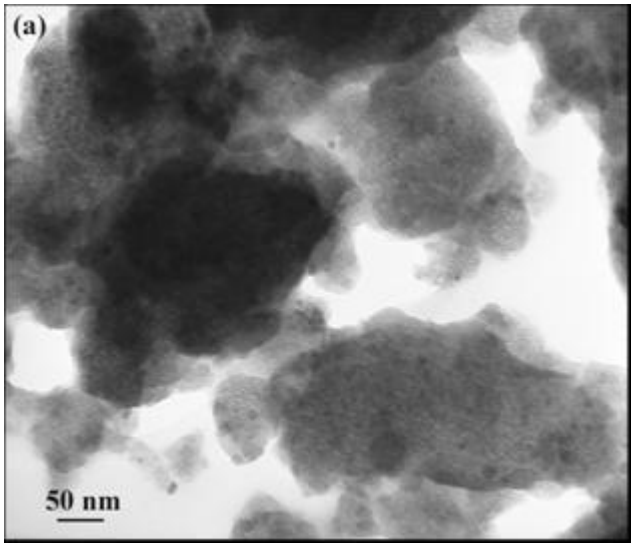

Figure 5b

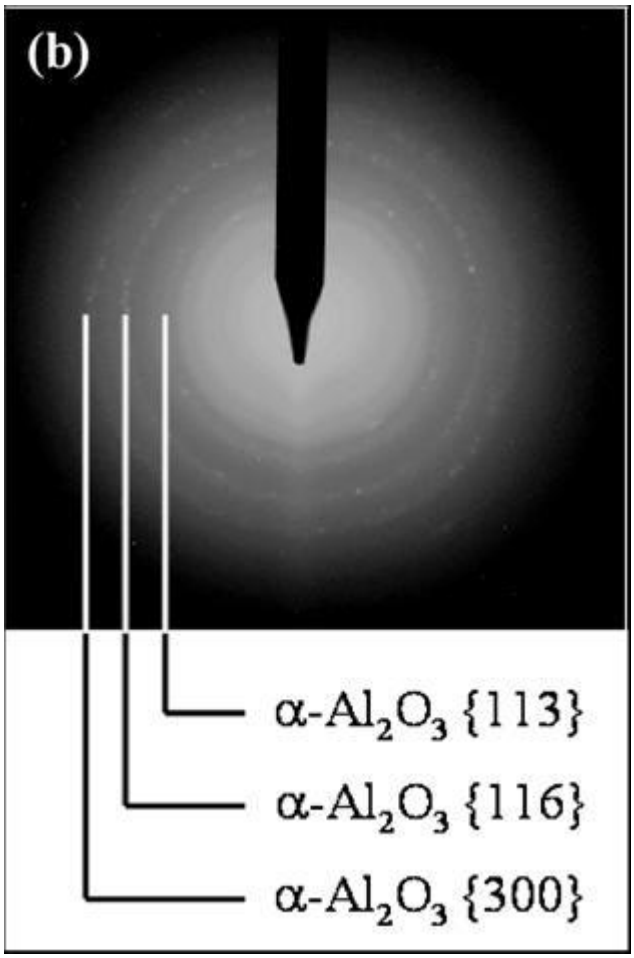

Figure 6

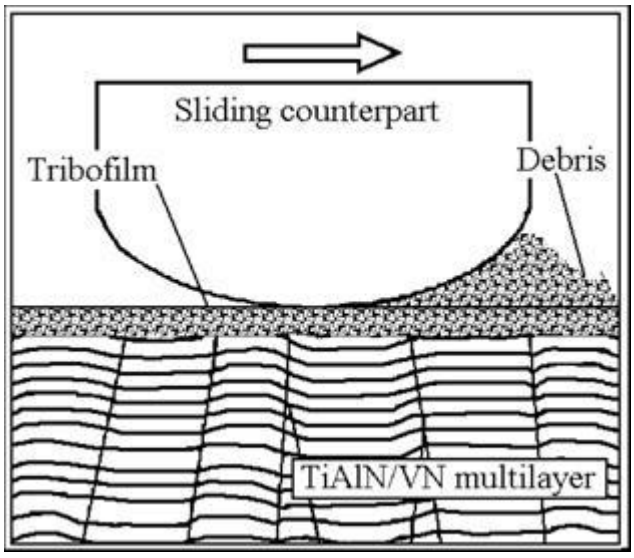
Sliding counterpart
Tribofilm
Debris
TiAlN/VN multilayer